Supporting Information

Nickel-catalyzed CNTs enhancing cycle performance of Si@C anodes

Zheng Wang[a, b, c], Shuling Liu[a*], Ming Li[b, c*], Bo sun[b, c], Hao Li[b, c], Haocheng Wen[b, c], Haoqi Li[b, c], Wenyu Liu[b, c], Ruotong Liu[b, c], Dongzhu Liu[b, c], Aoxiang Kou[b, c], Xifei Li[b, c*]

a Department of Chemistry and Chemical Engineering, Shaanxi Collaborative Innovation Center of Industrial Auxiliary Chemistry & Technology, Key Laboratory of Auxiliary Chemistry and Technology for Chemical Industry, Ministry of Education, The Youth Innovation Team of Shaanxi Universities, Shaanxi University of Science and Technology, Xi'an, Shaanxi 710021, P. R. China

b Institute of Advanced Electrochemical Energy & School of Materials Science and Engineering, Xi'an University of Technology, Xi'an 710048, PR China.

c Shaanxi Engineering Research Center of Key Materials for Lithium/Sodium-ion Batteries, Xi'an 710048, PR China.

*Corresponding Authors

E-mail address:

shulingliu@aliyun.com

xfli2011@hotmail.com; xfli@xaut.edu.cn

wsumolm@163.com

Supplementary Figures

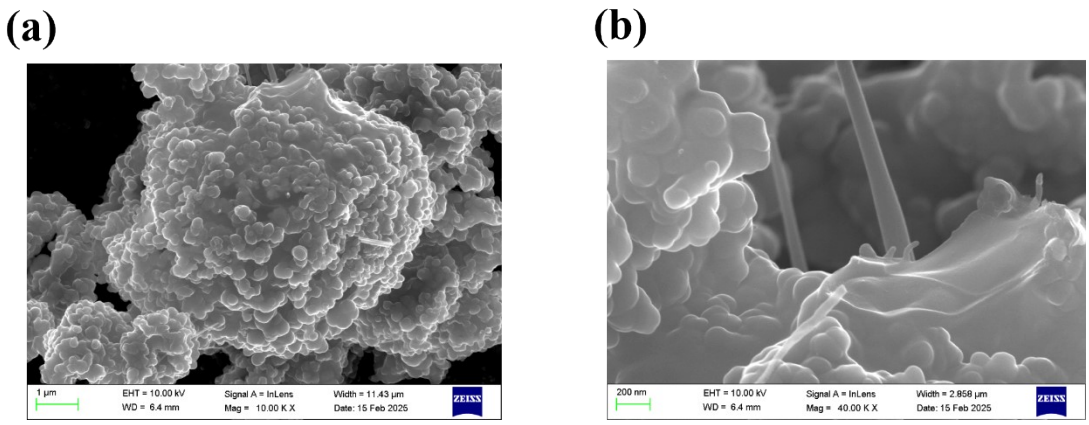

Figure S1. The SEM images of Si@N-C-CNTs@C.

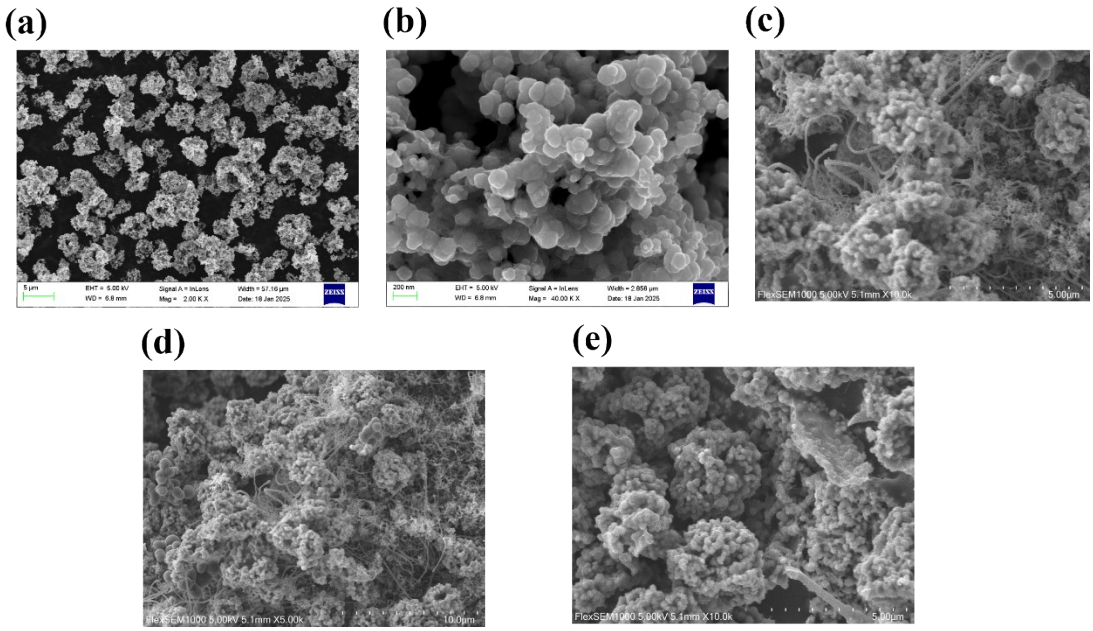

Figure S2. The SEM images of Si@N-C-CNTs.

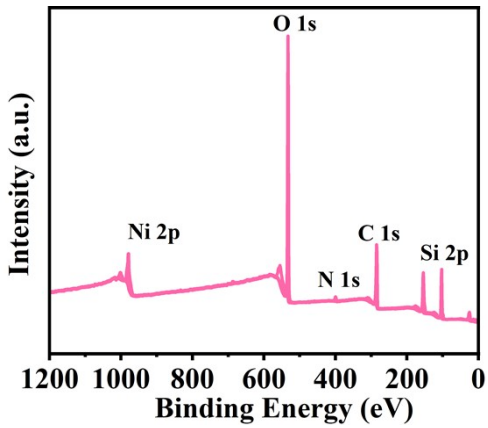

Figure S3. XPS patterns of Si@N-C-CNTs@C.

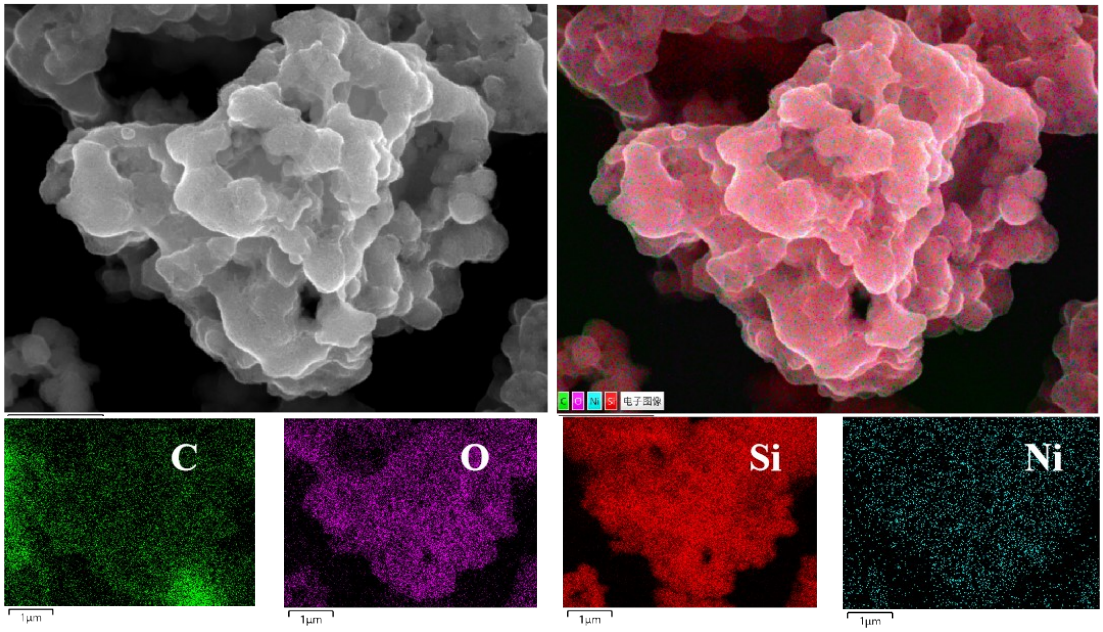

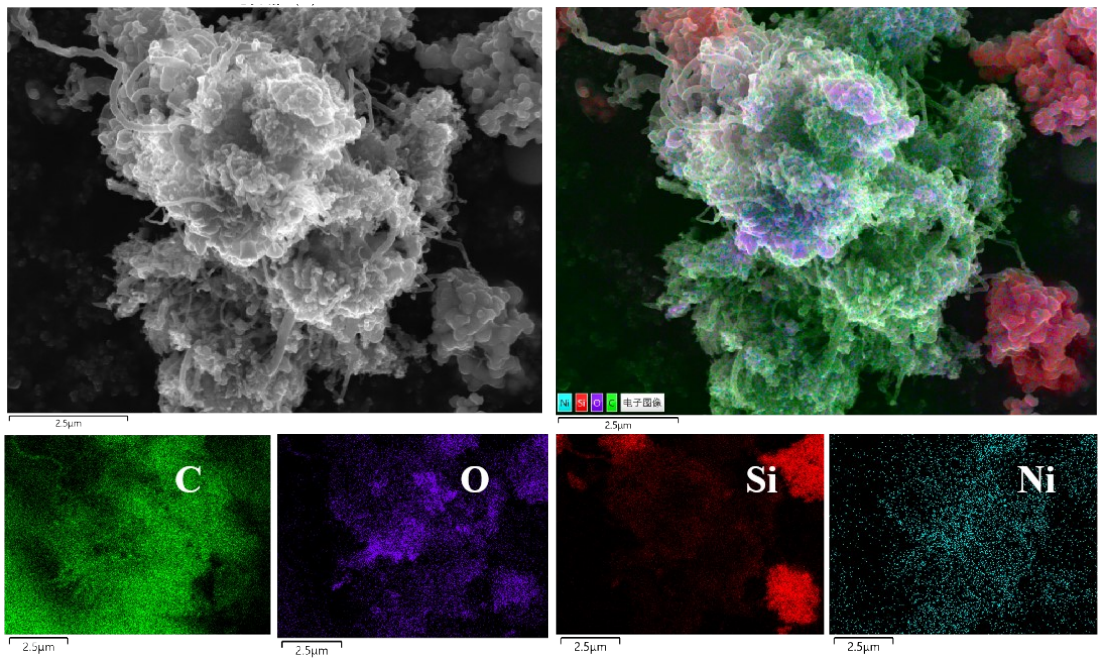

Figure S4. Elemental mapping images of the Si@N-C-CNTs@C-Mapping (SEM).

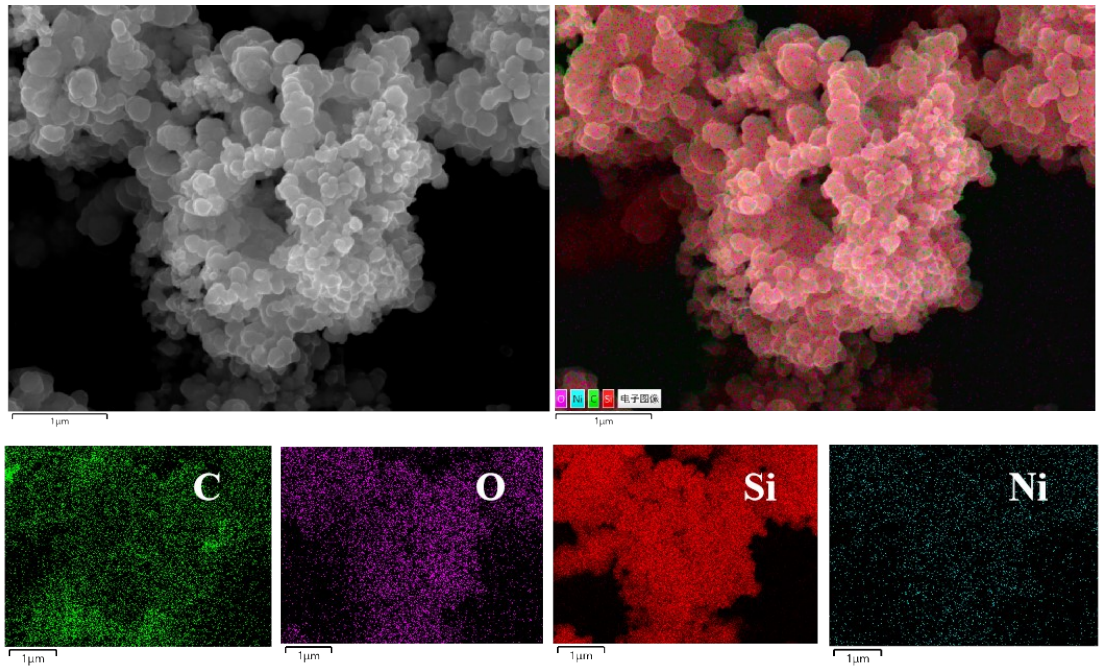

Figure S5. Elemental mapping images of the Si@N-C-CNTs-Mapping (SEM).

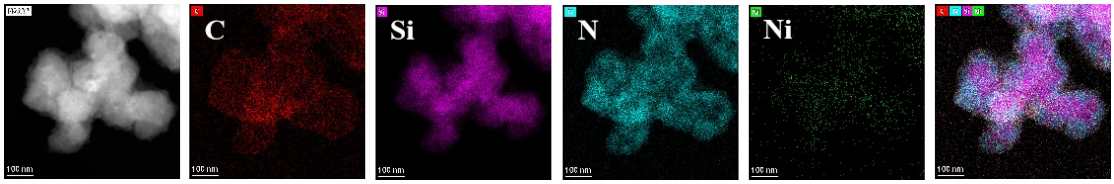

Figure S6. Elemental mapping images of the Si@N-C-CNTs-Mapping (TEM).

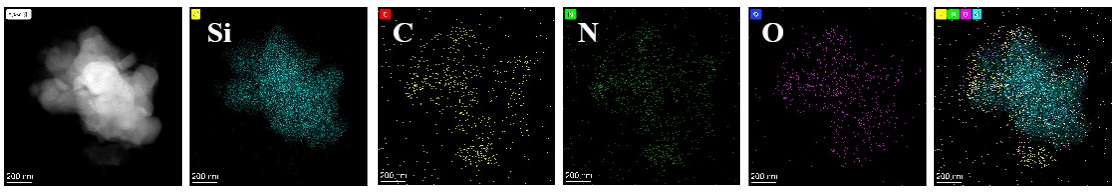

Figure S7. Elemental mapping images of the Si@N-C-Mapping (TEM).

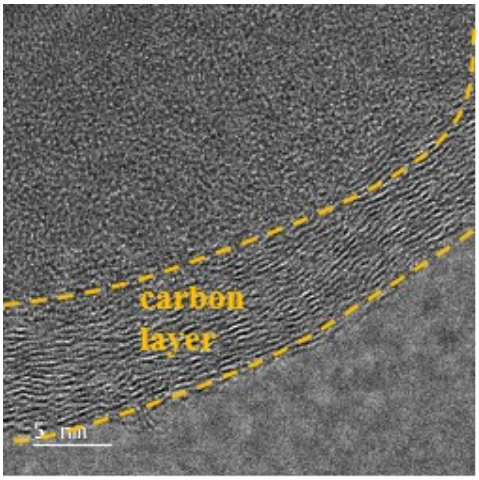

Figure S8. The TEM images of Si@N-C-CNTs@C.

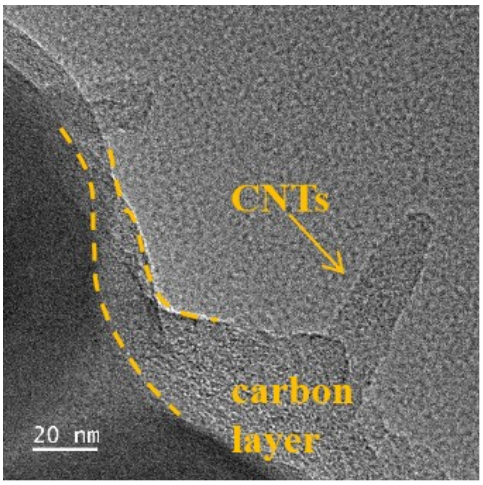

Figure S9. The TEM images of Si@N-C-CNTs@C.

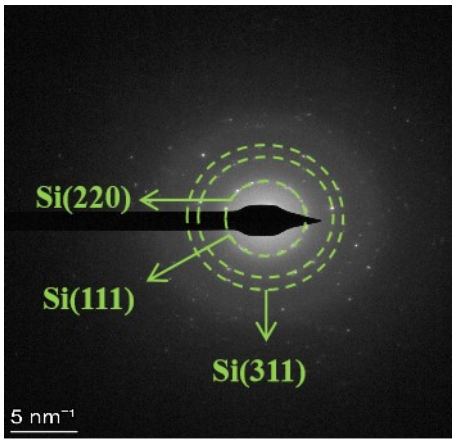

Figure S10. SAED images of Si@N-C-CNTs@C.

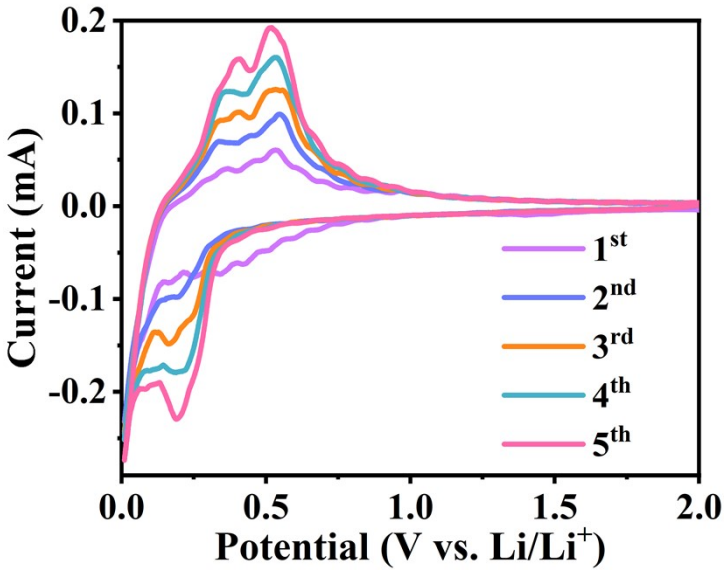

Figure S11. The CV curves of Si@N-C-CNTs.

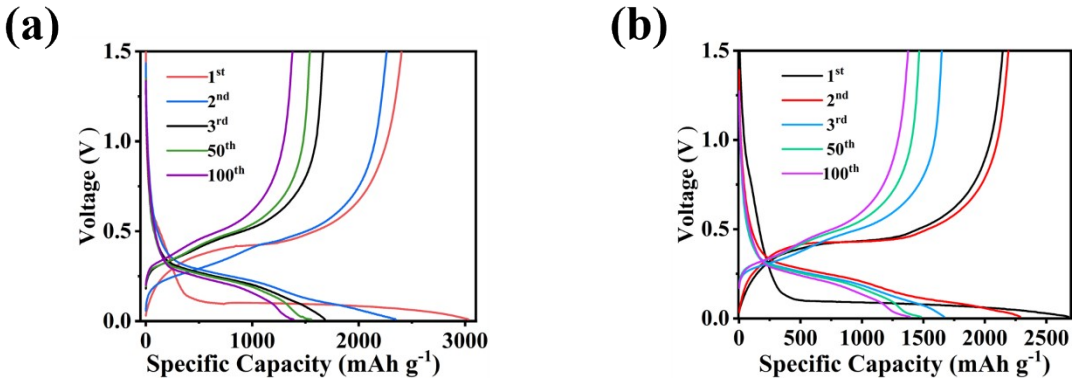

Fig.S12. (a) GCD curves at 2 A g^{-1} of Si@N-C-CNTs. (b) GCD curves at 2 A g^{-1} of Si@N-C-CNTs@C.

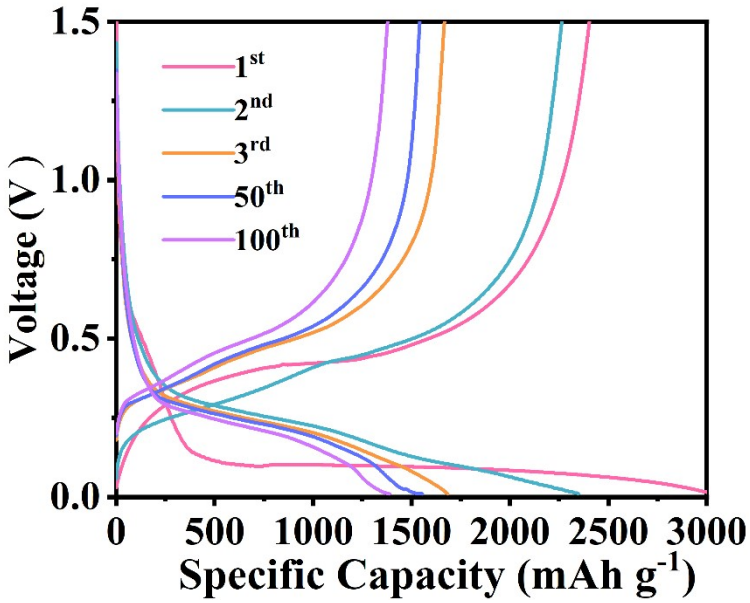

Fig.S13. (a) GCD curves at 1 A g^{-1} of Si@N-C-CNTs.

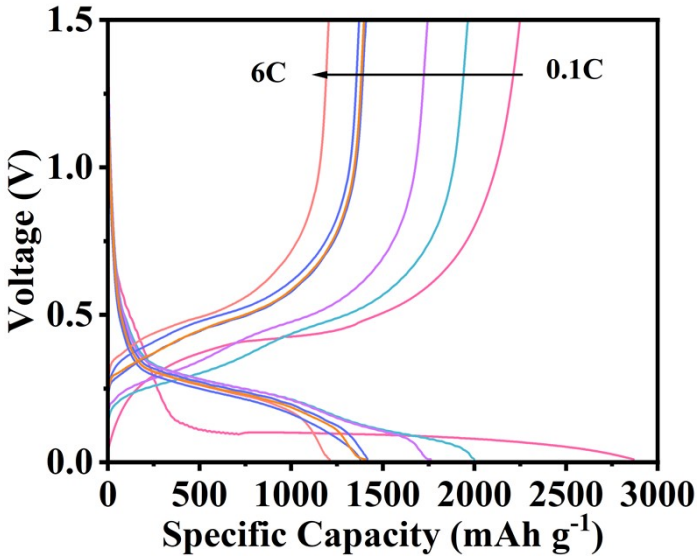

Fig.S14. The charge-discharge at different current density of Si@N-C-CNTs.

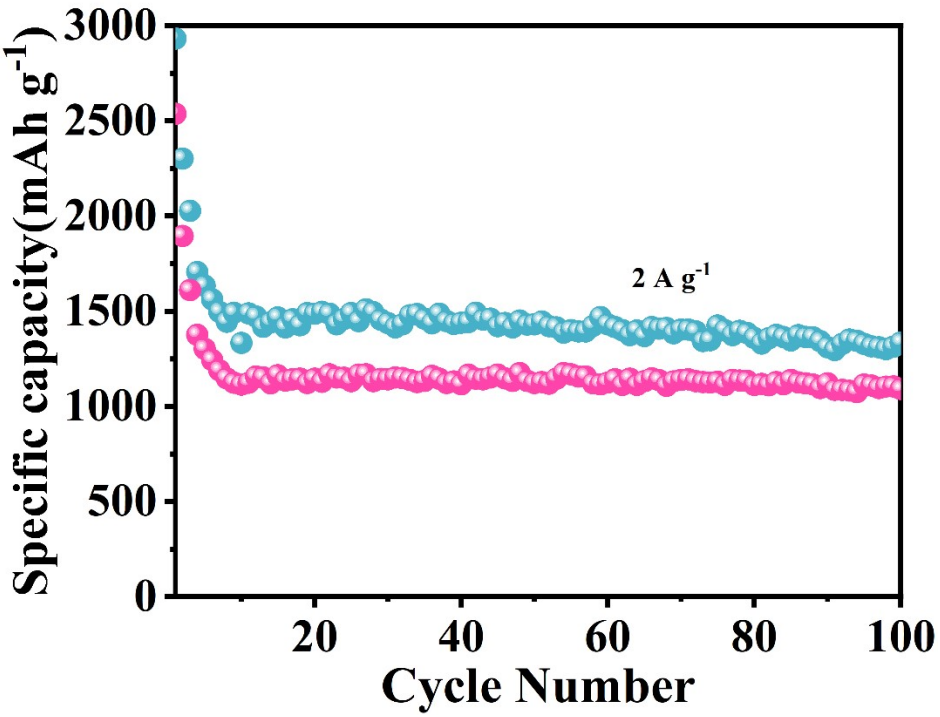

Figure S15. Cycling performance of Si@N-C-CNTs and Si@N-C-CNTs@C at 2 A g^{-1}.

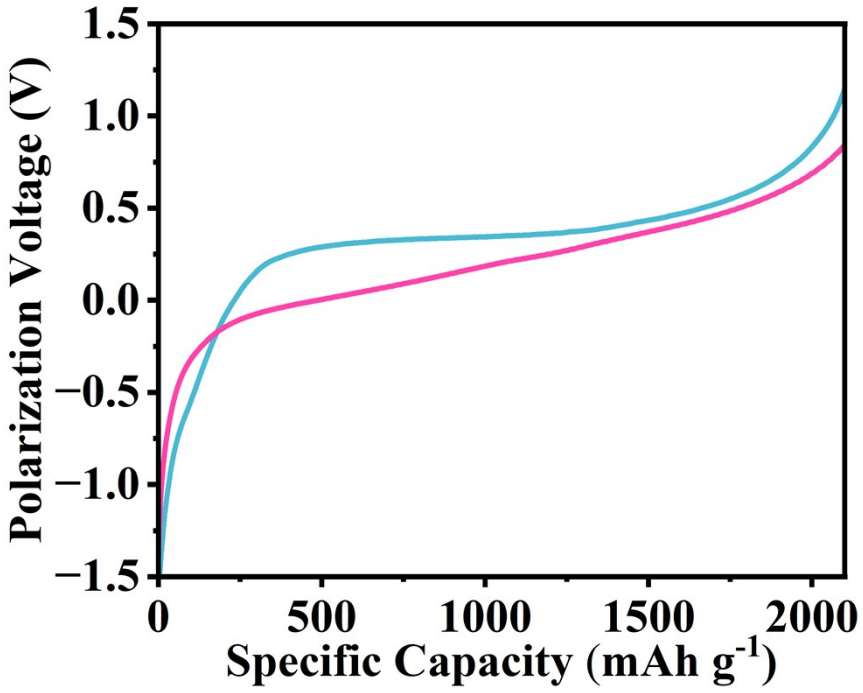

Figure S16. The polarization voltage corresponding to Si@N-C-CNTs and Si@N-C-CNTs@C.

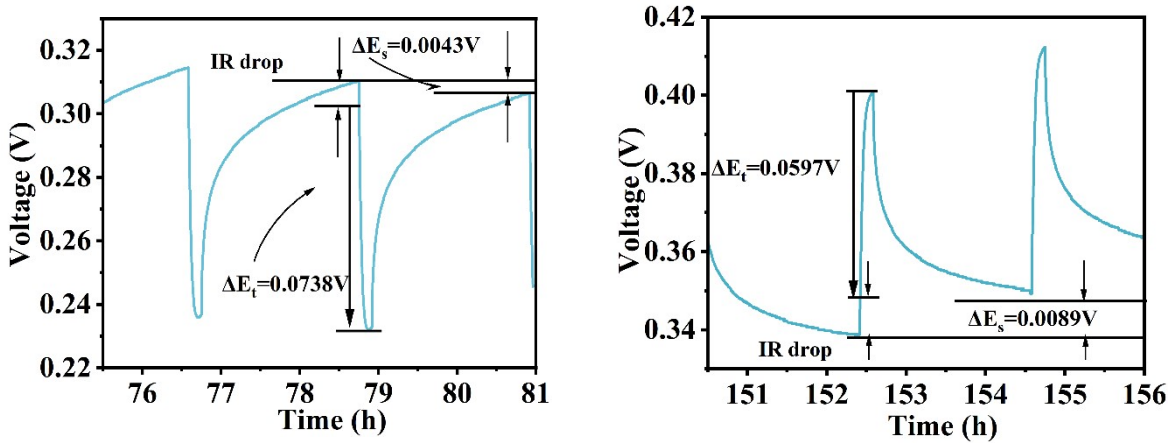

Figure S17. The GITT curves of Si@N-C-CNTs.

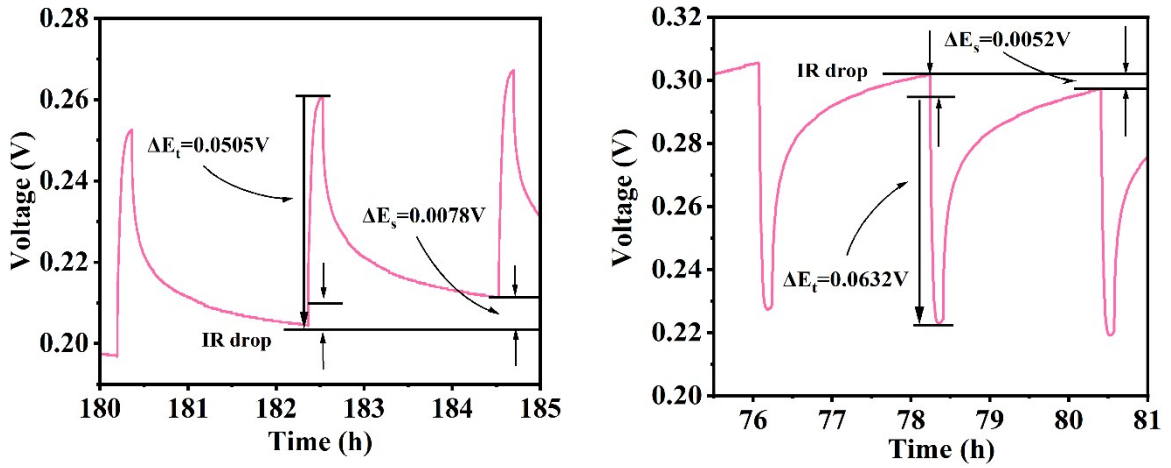

Figure S18. The GITT curves of Si@N-C-CNTs@C.

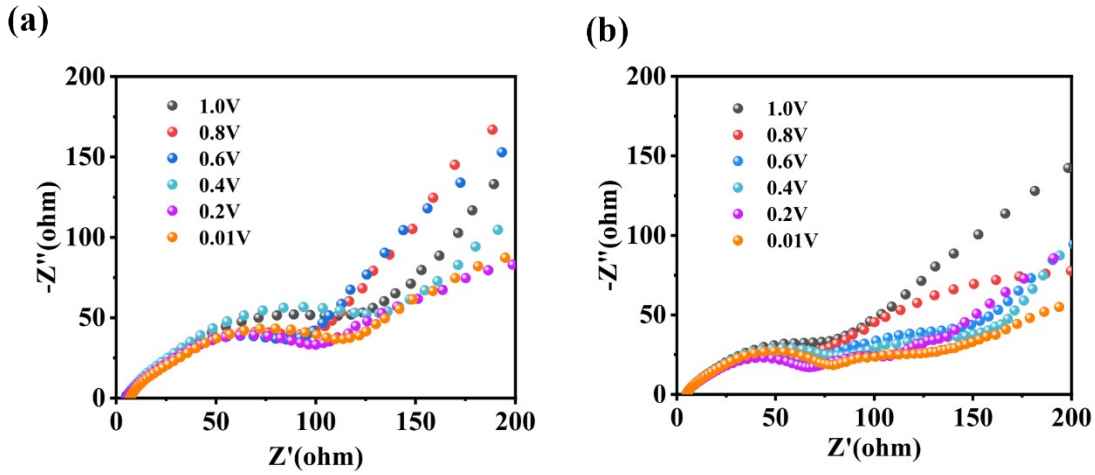

Figure S19. (a) Impedance spectra of Si@N-C-CNTs at different voltages. (b) Impedance spectra of Si@N-C-CNTs@C at different voltages.

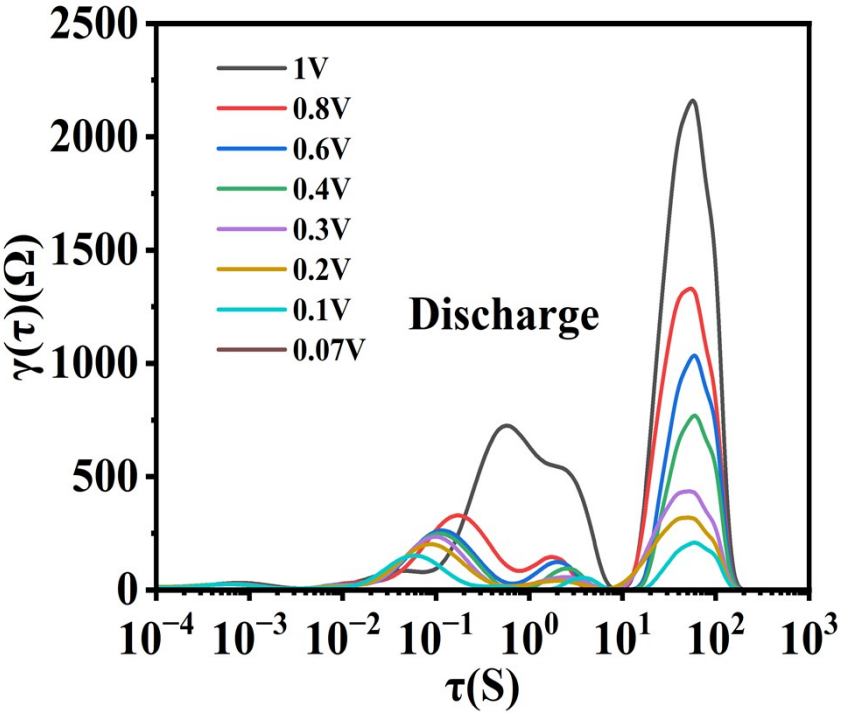

Figure S20. Enlarged view of DRT curves of in situ EIS spectra of Si@N-C-CNTs@C during the discharge

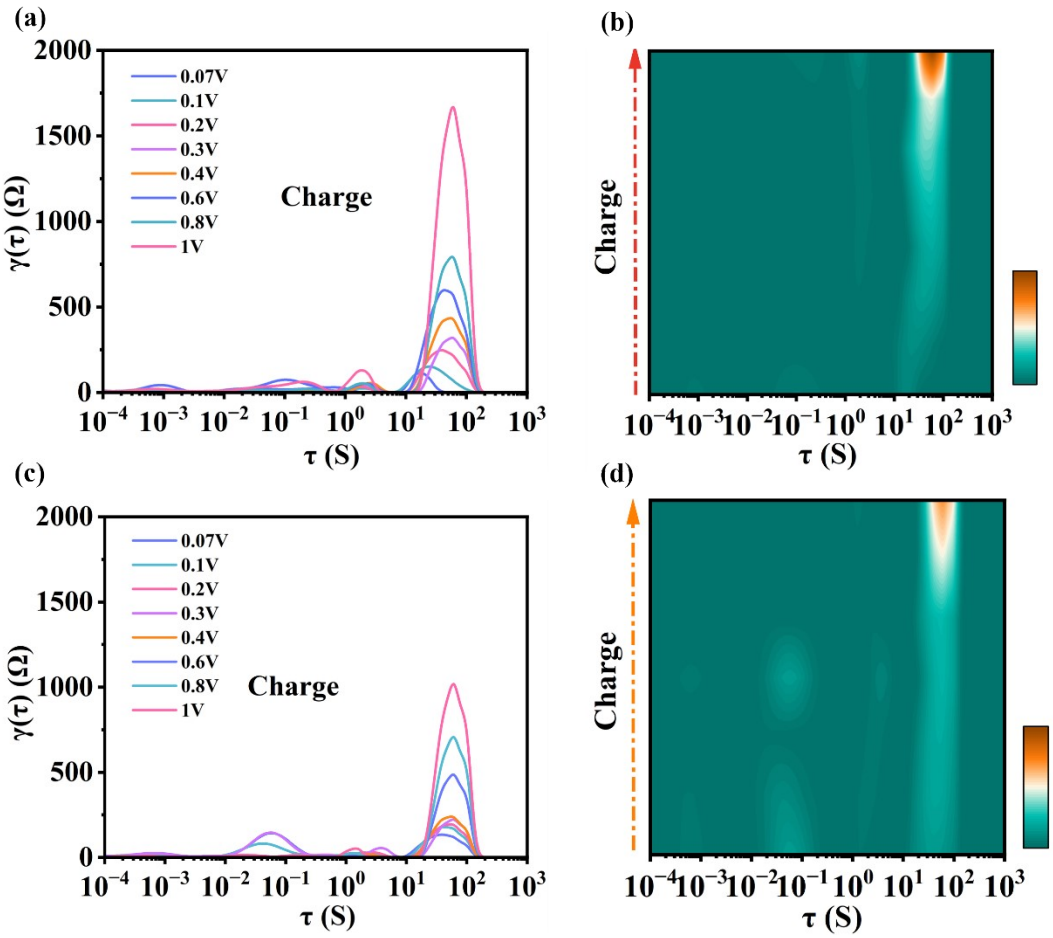

Figure S21. The DRT transformation of in situ EIS spectra for (a) Si@N-C-CNTs and (c) Si@N-C-CNTs@C during the charge. (b,d) DRT curves of in situ EIS spectra of Si@N-C-CNTs and Si@N-C-CNTs@C during the charge.

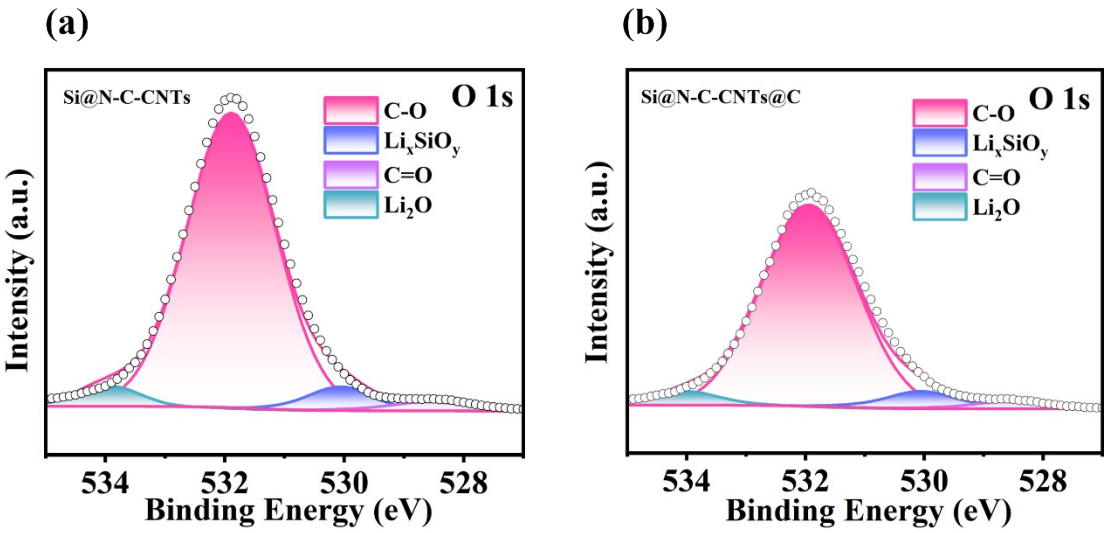

Figure S22. (a) O1s XPS patterns of Si@N-C-CNTs and (b) Si@N-C-CNTs@C

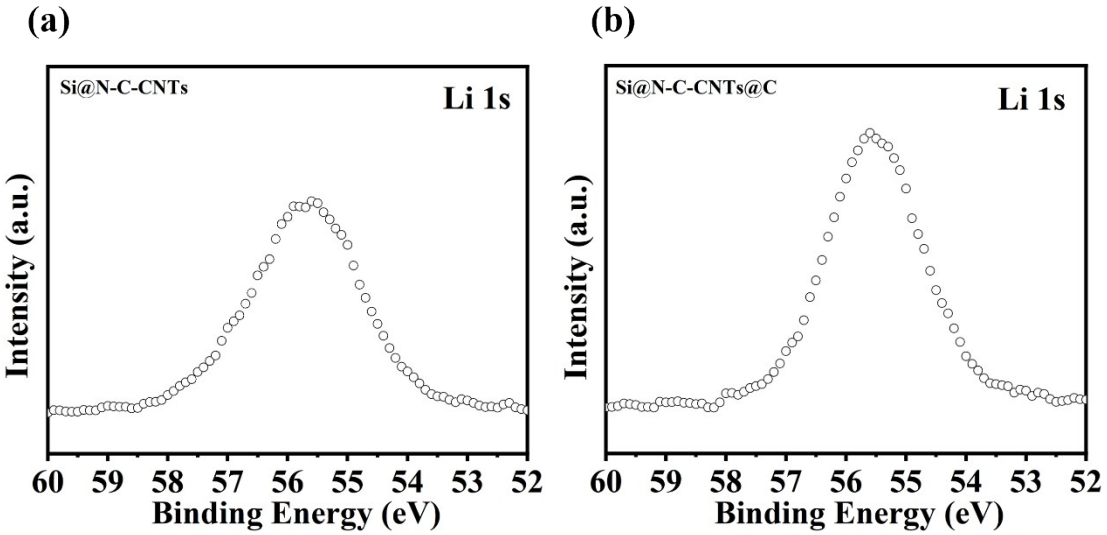

Figure S23. (a) Li 1s XPS patterns of Si@N-C-CNTs and (b) Si@N-C-CNTs@C

Table S1. Geometric parameters used in the finite element models.

Component	Dimension
Silicon core diameter	50nm
Carbon coating thickness	5nm
CNT diameter	10nm
CNT length	120nm
Dense carbon coating thickness	10nm

The geometric dimensions were based on typical experimental observations and are summarized in Table S1. The models were built in 2D axisymmetric or 3D space (the reports indicate a 2D geometry, possibly axisymmetric). The silicon core was modeled as a sphere of 50 nm diameter, surrounded by a 5 nm carbon coating. Carbon nanotubes (CNTs) were represented as cylindrical structures with a diameter of 10 nm and a length of 120 nm, attached to the carbon-coated silicon surface. For the Si@N-C-CNTs@C model, an additional dense carbon layer of 10 nm thickness was added encapsulating the entire Si@N-C-CNTs unit. All geometric units were set to nanometers (nm).

Table S2. Material properties assigned to each domain in the COMSOL

Material	Young's modulus (GPa)	Poisson's ratio
Si	100	0.3
Carbon	10	0.3
CNTs	200	0.25

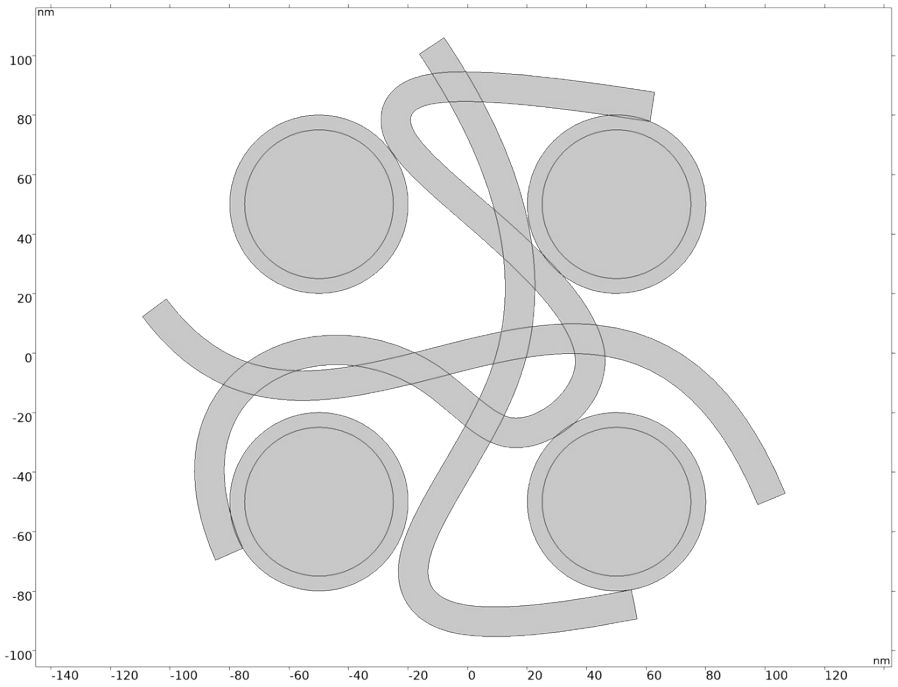

Figure S24. Initial finite element model design of Si@N-C-CNTs.

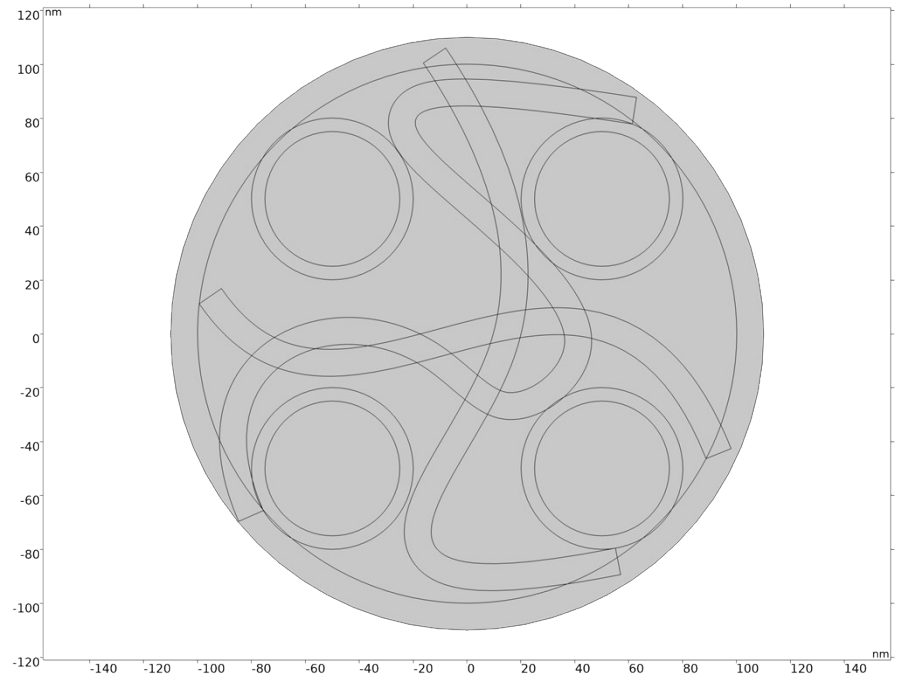

Figure S25. Initial finite element model design of Si@N-C-CNTs@C.